

Transport properties and spin disorder in the degenerate ferro-spin-glass $\text{Sn}_{1-x}\text{Mn}_x\text{Te}$

A. Mauger

*Groupe de Physique des Solides de l'École Normale Supérieure, Université Paris 7, 2 place Jussieu,
75251 Paris Cedex 05, France*

M. Escorne

*Laboratoire de Physique des Solides, et Laboratoire de Chimie Métallurgique des Terres Rares, 1 place Aristide-Briand,
92190 Meudon, France*

(Received 9 April 1986)

We have investigated the resistivity ρ of $\text{Sn}_{1-x}\text{Mn}_x\text{Te}$ solid solutions for various manganese concentrations in the range $x < 0.07$, as a function of temperature in the range $1.5 < T < 15$ K. The data include the paramagnetic, ferromagnetic, and reentrant spin-glass regions of the phase diagram in the x - T plane. We argue that the thermal dependence of ρ is due to the incoherent potential plus exchange scattering from the Mn ions. A very good agreement is found with the Koon-Schindler-Mills model, provided that magnetic clustering effects are taken into account. It is shown that the free-carrier mean free path $\lambda \sim 200$ Å is smaller than the ferromagnetic cluster size, so that the transport properties can be used as a probe of local magnetic properties at a microscopic scale. In particular, we show that the lowering of the bulk magnetization in the reentrant phase is compensated for by an increase of the local magnetization inside the ferromagnetic clusters.

I. INTRODUCTION

The physical effects associated to magnetic impurities are currently the subject of considerable interest. The first studies on this subject concern the case of $3d$ impurities (Fe, Mn, Cr) diluted in noble metals (Cu, Ag, Au).^{1,2} More recently, spin-glass properties first discovered in these materials have also been observed when these magnetic impurities are diluted in semiconductors such as II-VI compounds, which, actually, are insulators at the low temperatures where the spin freezing takes place.³ Between these two extreme cases, there is a possibility to dilute these magnetic impurities in semiconductors with a density of acceptors or donors which exceeds the critical Mott concentration for the metal-insulator transition so that these materials remain degenerate down to the lowest temperature. $\text{Sn}_{1-x}\text{Mn}_x\text{Te}$ is a good example⁴ with a low-density free-carrier gas $10^{20} < p < 5 \times 10^{20}$ cm⁻³ presumably due to Sn vacancies.⁴

In Sec. II of this paper, we first recall the basic magnetic properties of $\text{Sn}_{1-x}\text{Mn}_x\text{Te}$ investigated in detail elsewhere⁵⁻⁷ and focus attention to those of the magnetic properties which are specific to the existence of the low-density free-carrier gas. Then, in Sec. III, we report resistivity measurements which evidence sharp variations of the spin-disorder resistivity as a function of temperature in agreement with the data from magnetic experiments. We find that the spin-disorder resistivity cannot be described by the oversimplified model of Ghazali *et al.*⁸ for the same material, but a very good agreement with experiment is found within the model developed by Koon *et al.*⁹ to fit resistivity curves of Pd:Fe alloys. The results corroborate our previous analysis on the nature of the exchange interactions and spin freezing in $\text{Sn}_{1-x}\text{Mn}_x\text{Te}$.

II. MAGNETIC PROPERTIES

The magnetic properties of $\text{Sn}_{1-x}\text{Mn}_x\text{Te}$ alloys have been explored earlier.⁴⁻⁷ At low temperatures, the saturation moment of the magnetization curve in the high-field limit is $5\mu_B$. In the paramagnetic configuration, the magnetic susceptibility satisfies the Curie-Weiss law with a magnetic moment also in agreement with the theoretical value predicted for Mn^{2+} ions in the $(3d)^5S_{5/2}$ configuration. A synthesis of the results is provided by the magnetic phase diagram in Fig. 1. The system is a good spin glass for Mn concentrations $x < 3$ at. %, but at larger concentrations, a ferromagnetic phase is observed, characterized by the existence of a spontaneous magnetization in low magnetic fields, in a definite range of temperatures, below the Curie temperature T_C .⁷ At lowest temperature, a reentrant spin-glass phase is observed, characterized by an increase of irreversible effects.^{5,6} The existence of a ferromagnetic long-range ordering down to Mn concentrations as small as 3 at. % suggests the existence of a long-range magnetic interaction, namely the Ruderman-Kittel-Kasuya-Yosida indirect exchange mediated via the few 10^{20} holes present in the samples.

We assume that the Hamiltonian which couples the local spin \mathbf{S}_n carried by the Mn^{2+} ion at site R_n with the spin density $s(r)$ of the free carriers is local:

$$H_{\text{ex}} = - \sum_n J \mathbf{S}_n \cdot \mathbf{s}(R_n) \quad (1)$$

with J the exchange constant. To second order in perturbation, we obtain the RKKY interaction:

$$H'_{\text{ex}} = - \frac{1}{2} \sum_{i,j} J_{\text{eff}}(\mathbf{R}_{ij}) \mathbf{S}_i \cdot \mathbf{S}_j \quad (2)$$

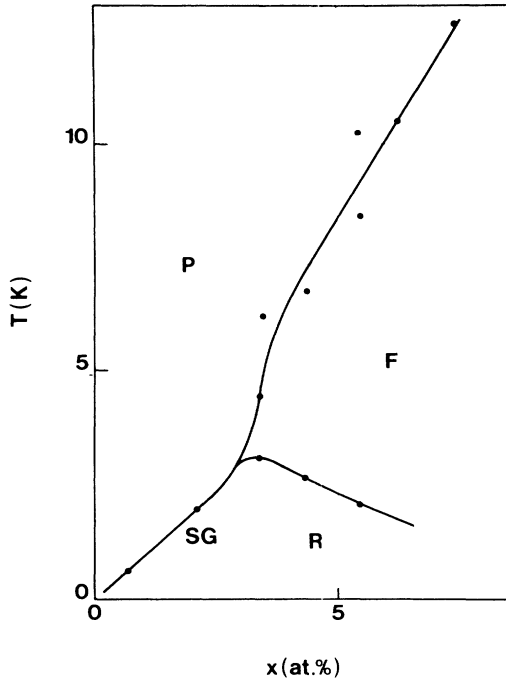


FIG. 1. Magnetic phase diagram of $\text{Sn}_{1-x}\text{Mn}_x\text{Te}$ after Refs. 5 and 6. *P* is the superparamagnetic phase. *F* is the ferromagnetic phase where ferromagnetic clusters coexist with a long-range magnetic order. *SG* is the spin-glass phase, *R* denotes the reentrant spin-glass phase.

with the effective exchange coupling

$$J_{\text{eff}}(R_{ij}) = \frac{1}{2} \left(\frac{J}{N} \right)^2 \sum_{\mathbf{q}} \chi^0(\mathbf{q}) e^{i\mathbf{q} \cdot \mathbf{R}_{ij}}, \quad (3)$$

$\chi^0(\mathbf{q})$ is the susceptibility of the free-carrier gas:⁸

$$\chi^0(\mathbf{q}) = - \sum_{\mathbf{k}} \frac{n_{\mathbf{k}}}{E(\mathbf{k}) - E(\mathbf{k} + \mathbf{q})} \quad (4)$$

and N is the number of unit cells. For a parabolic dispersion relation of the hole gas, $E(k) = \hbar^2 k^2 / 2m^*$, $\chi^0(q)$ can be calculated explicitly¹⁰ to give

$$J_{\text{eff}}(\mathbf{R}_{ij}) = \frac{3p}{8E_F} \left(\frac{J}{N} \right)^2 \sum_{\mathbf{q}} H(\mathbf{q}) e^{i\mathbf{q} \cdot \mathbf{R}_{ij}} \quad (5)$$

with $H(q)$ the Lindhart function:¹¹

$$H(\mathbf{q}) = 1 + \frac{4k_F^2 - q^2}{4k_F q} \ln \left| \frac{q + 2k_F}{q - 2k_F} \right|, \quad (6)$$

p is the hole concentration, k_F the wave vector of the holes at the Fermi energy E_F . In the molecular-field approximation (MFA) which will be discussed hereafter, the RKKY interaction leads to a magnetic ordering at the temperature

$$T_c = \frac{2S(S+1)}{3k_B} J_{\text{eff}}(Q) \quad (7)$$

with Q the wave vector q of the magnetic structure, defined by the q value for which

$$J_{\text{eff}}(\mathbf{q}) = \sum_j J_{\text{eff}}(\mathbf{R}_{ij}) e^{i\mathbf{q} \cdot \mathbf{R}_{ij}} \quad (8)$$

is a maximum.

Equations (1)–(6) are classical expressions of the RKKY interaction, independent of the localized spin concentration x . The effect of this interaction, however, strongly depends on x . For a single magnetic impurity ($x \rightarrow 0$), the summation over q in Eq. (5) leads to

$$J_{\text{eff}}(R_{ij}) = \frac{9\pi}{2} \frac{p^2}{E_F} J^2 \frac{\sin(2k_F R_{ij}) - 2k_F R_{ij} \cos(2k_F R_{ij})}{(2k_F R_{ij})^4}. \quad (9)$$

This equation shows that the spin polarization of the free carrier $s(r) \propto J_{\text{eff}}(r)$ creates a ferromagnetic cloud which extends to a distance

$$R \sim \pi / (2k_F). \quad (10)$$

At larger distances, $s(r)$ and $J_{\text{eff}}(r)$ present Friedel-type oscillations. In the opposite case $x \rightarrow 1$ which is met in magnetic semiconductors (such as europium chalcogenides) and rare-earth metals, the localized spins S_j are distributed on a periodic array which lead to coherent interference effects between the Friedel oscillations in Eq. (9). Therefore the summation over j in Eq. (8) is an oscillating function of k_F . These well-known RKKY oscillations depend on the topology of the lattice and have been studied in detail¹² at least in cubic lattices. Such oscillations of $J_{\text{eff}}(q)$ versus k_F for all q (and in particular for $q=0$) are expected to smear out as x decreases from unity, because the coherence of the interference between the Friedel oscillations will disappear when the periodic arrangement of the localized spins on the lattice will be altered by the dilution process. On a mathematical point of view, this loss of spatial ordering in the distribution of the magnetic ions means that the discrete summations over the lattice can be averaged by integrals in the preceding equations:

$$\sum_j \rightarrow \int d\mathbf{r}. \quad (11)$$

Since the lattice is defined by the atomic positions inside a unit cell, i.e., the position of nearest neighbors (NN), we expect that the RKKY oscillations will disappear basically for a magnetic impurity concentration the order of magnitude of the geometric site percolation concentration of the lattice for NN interactions, x_p . It is important to realize that the condition of validity ($x < x_p$) for the jellium approximation [Eq. (11)] is a problem in geometric disorder. In particular, the restriction to NN simply defines x_p as the *geometric* percolation threshold, and does not involve any hypothesis on the range of the magnetic interactions between magnetic impurities. Actually, one can define independently a *magnetic* percolation concentration x_c above which long-range magnetic ordering takes place at a finite temperature. Of course, if the magnetic interactions are restricted to NN, then $x_c = x_p$, but if the interaction Hamiltonian between the magnetic moments is long range (which is the present case for RKKY interactions), x_c is substantially smaller than x_p .

We show how one can derive both the nature of the magnetic ordering for $x > x_c$, and an estimation of x_c . For $x < x_p$, the Friedel oscillations will interfere incoherently and will then average to residual local fluctuations $\Delta E(r)$ of the exchange interaction. In this case the RKKY interaction mainly consists in the ferromagnetic interaction, the range of which is given by Eq. (10).

If R is larger than the mean distance \bar{R} between the magnetic ions, the ferromagnetic clouds around the magnetic ions will overlap, driving a transition to a ferromagnetic phase at a Curie temperature T_C . Since the mean volume occupied by the magnetic impurities is

$$\frac{4}{3} \pi \bar{R}^3 = \frac{\Omega}{x} \quad (12)$$

with Ω the volume of the unit cell, the condition $R > \bar{R}$ writes $x < x_c$, with x_c the critical concentration

$$x_c \sim \frac{18}{\pi^2} \Omega p. \quad (13)$$

For $x > x_c$ the MFA can be used and T_c is given by Eqs. (7) and (8), with $Q=0$. For $x < x_p$, the jellium approximation [Eq. (11)] can be used to evaluate $\sum_j J_{\text{eff}}(\mathbf{R}_{ij})$, in which case Eq. (5) leads to the following:

$$\sum_j J_{\text{eff}}(\mathbf{R}_{ij}) \rightarrow \frac{3p}{8E_F} \left[\frac{J}{N} \right]^2 H(q=0). \quad (14)$$

Since $x_c < x_p$, there is a whole range of concentrations $x_c < x < x_p$ where both Eqs. (7) and (14) can be used to derive T_c . Since $H(q=0)=2$ according to Eq. (6), the Curie temperature is given by

$$T_C = \frac{S(S+1)}{4k_B} J^2 \Omega \frac{px}{E_F}, \quad x_c \leq x \leq x_p. \quad (15)$$

This is the expression already derived in Ref. 8 in a different way, to which we have now added the limit of validity. Therefore in this range of Mn concentrations, T_C does not oscillate as a function of k_F or p , but just increases monotonically like $p^{1/3}$.

In the opposite case $\bar{R} > R$, the ferromagnetic interaction due to the ferromagnetic clouds around any given localized spin is not experienced by the other localized spins which are now too remote, with the consequence that the ferromagnetic long-range ordering is broken.

In this case, a spin-glass freezing will be observed at a temperature T_g where the exchange interaction J_{eff} between localized spins distant by the mean distance \bar{R} will balance the thermal energy:

$$|J_{\text{eff}}(\bar{R})| \simeq k_B T_g. \quad (16)$$

Since $\bar{R} > R$, this exchange interaction is the tail of the RKKY interaction, i.e., the oscillation part, which decreases like R^{-3} ; taking Eq. (12) into account, we get the scaling law:¹³

$$T_g \propto x, \quad x < x_c. \quad (17)$$

Since $T_g = T_c$ for $x = x_c$, Eq. (17) implies that $T_g(x)$ is just the linear curve $T_c(x)$ given by Eq. (15) extrapolated in the range $0 < x < x_c$.

Let us now compare these results with the phase diagram in Fig. 1. For all samples investigated, $x < x_p$ since $x_p \sim 0.3$ is above the limit of solubility of Mn in SnTe. The linear law of T_c versus x in Eq. (15) is in quite good agreement with experiment (except in the close vicinity of $x = x_c$ where the MFA is not a good approximation and where correlations must be taken into account). Other calculations, in the mean-random-field theory¹⁴ reproduce the same results. The linear dependence of T_g versus x is also approximately satisfied. Note that the mean-random-field theory predicts a different behavior^{14,15} ($T_g \propto x^\alpha$ with $0.5 < \alpha < 0.66$). Since we have only two experimental points in the range $x < x_c$, this x dependence cannot be ruled out although the data are in closer agreement with Eq. (17). For the samples we have studied, the hole concentration deduced from Hall-effect measurements, taking the anisotropy factor 0.6 into account¹⁶ give $p \sim 5 \times 10^{20} \text{ cm}^{-3}$. Assuming that the variation of the lattice parameter with x is negligible for these low Mn concentrations, Eq. (15) gives $x_c \simeq 5$ at. %, which reproduces quite well the order of magnitude of the experimental value $x_c \simeq 3$ at. %. This result is thus a proof of our previous assumptions⁶ that the ferromagnetic ordering for $x > x_c$ originates from the ferromagnetic cloud around magnetic impurities, while the spin-glass freezing for $x < x_c$ is due to the oscillating tail of the RKKY interaction, like in metallic spin glasses. Since $T_{c,g} \propto p^{1/3}$, the lines $T_{c,g}(x)$ in the phase diagram (Fig. 1) do not depend strongly on the hole concentration. In particular, the comparison between the experimental and theoretical slopes of the curves $T_c(x)$ gives a determination of the parameter J :

$$J = 0.4 \text{ eV}. \quad (18)$$

The critical point of the phase diagram, however, is located at coordinates directly proportional to p according to Eq. (14). It follows that its location in Fig. 1 is not a specific property of the material, but results from the fact that our samples were prepared with a concentration $p \sim 5 \times 10^{20} \text{ cm}^{-3}$ Sn vacancies.

III. TRANSPORT PROPERTIES

Transport properties of $\text{Sn}_{1-x}\text{Mn}_x\text{Te}$ have been previously investigated in Ref. 7 for $x > 3$ at. %, in the vicinity of the Curie temperature.⁸ In the range of interest ($T < 10$ K), the resistivity of the host matrix SnTe does not depend on temperature, so that the diffusion of the holes by phonons is negligible. Therefore, the variations of ρ with temperature in $\text{Sn}_{1-x}\text{Mn}_x\text{Te}$ for $T < 10$ K is due to the scattering of the holes by the magnetic impurities.

We have reported in Fig. 2 the temperature dependence of the resistivity for Mn concentrations $x > 3$ at. % in the range $2 < T < 10$ K. In agreement with previous results, the ferromagnetic ordering at the Curie temperature T_c induces a decrease of the resistivity. T_c , deduced from the zero-field magnetic susceptibility,^{5,6} illustrated in Fig. 1, coincides with experimental uncertainties with the inflection point of the resistivity curve, which is the canonic behavior in diluted ferromagnets, like PdFe.⁹ Note, however, that the freezing temperature T_c^f deduced from mag-

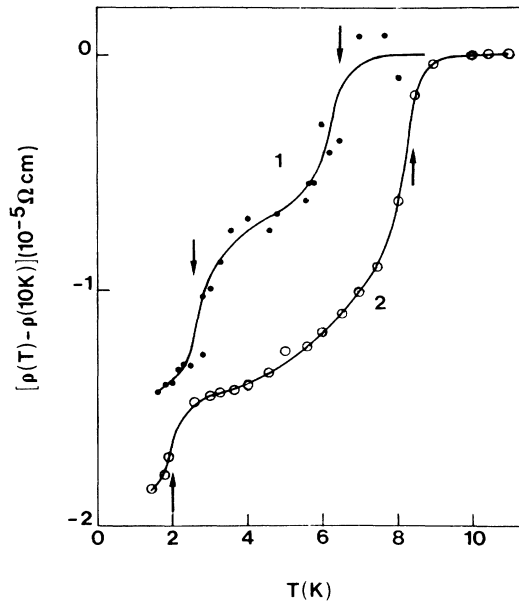


FIG. 2. Variations of the electrical resistivity ρ with temperature for two Mn concentrations $x=0.04$ [solid circles (1)] and $x=0.054$ [open circles (2)]. The solid lines are theoretical. The absolute value at $T=10$ K is reported in Fig. 4. Arrows mark the Curie and the reentrant phase temperatures.

netic susceptibility and magnetization data in a static external field $H \approx 100$ G is larger than T_c ,⁷ and rather corresponds to the temperature above which the resistivity becomes temperature independent. (It means, in particular, that there has been an incorrect confusion between T_c and T_c^f in Ref. 7.) This effect is due to the formation of ferromagnetic clusters in the range $T_c < T < T_c^f$. In this intermediate superparamagnetic phase, the interaction between these clusters is very weak so that the clusters give rise to a part of the magnetization easily saturated in a small applied field $H \sim 100$ G,⁶ corresponding to the Langevin-like magnetization associated to the orientation of these clusters along the external field. Therefore, the appearance of this magnetization at $H=100$ G corresponds to the onset of ferromagnetic clustering at T_c , which is distinct from the Curie temperature T_c defined as the temperature at which appears a spontaneous magnetization at zero field, associated to the blocking of the large ferromagnetic clusters to give a long-range ferromagnetic ordering. The decrease of ρ at T_c^f is evidence that the holes are sensitive to the ordering of the spins inside the ferromagnetic clusters. Since the resistivity only depends on the spin correlation at the scale of the mean free path of the hole, λ , this result implies that λ is smaller than the size of the magnetic clusters. Note also that the application of the field $H \sim 100$ G, which produces the rapid increase of the magnetization mentioned above, does not affect the resistivity [except that it suppresses the peak in $\rho(T)$ observed in some samples,⁸ in the intermediate superparamagnetic phase]. This is another form of evidence that λ is smaller than the size of the ferromagnetic clusters: the holes are a probe of the short spin correlations inside the clusters, and do not probe the mac-

roscopic bulk magnetization which depend on the domain structure and relative orientations of the ferromagnetic clusters. Above T_c , a similar situation has been met, for example, in Au-Fe alloys with Fe concentrations exceeding the value x_c appropriate for this system.¹⁷ Below T_c , however, the transport properties of $\text{Sn}_{1-x}\text{Mn}_x\text{Te}$ are markedly different from those of Au-Fe, in which the ferromagnetic phase is homogeneous.¹⁷ Actually the archetypal ferro-spin-glasses like Au-Fe,¹⁸ Cu-Mn,¹⁹ or Ni-Mn,²⁰ are homogeneous, which means that the microscopic properties at the scale of λ are essentially identical to those of the macroscopic samples, with a magnetoresistance which decreases quadratically as a function of the bulk magnetization M . The extension of this quadratic behavior suggests that in an homogeneous ferromagnetic configuration or a reentrant spin-glass phase, the spontaneous drop in resistivity upon cooling is also given by a quadratic law

$$\rho(T) = \rho_{\text{dis}} - \alpha M_0^2(T), \quad (19)$$

with ρ_{dis} the disordered state resistivity in the paramagnetic state, and M_0 the spontaneous magnetization. This law is indeed well verified in concentrated Au-Fe alloys,¹⁷ but our results show that it is not verified in $\text{Sn}_{1-x}\text{Mn}_x\text{Te}$. The most outstanding deviation with respect to the law occurs at the temperature T_r which separates the ferromagnetic phase from the reentrant spin-glass phase. The breakdown of the long-range ferromagnetic ordering tends to reduce the spontaneous magnetization M_0 which either collapses at T_r , according to the scaling laws,²¹ or at most stays constant like in Ni-Mn.²² In $\text{Sn}_{1-x}\text{Mn}_x\text{Te}$, we observe that the reentrance in the spin-glass phase at T_r induces a decrease of the resistivity, which is just the opposite behavior with respect to the predictions of Eq. (19).

A. Analysis

The diffusion cross section of the carriers by the magnetic impurities can be divided in two parts: (i) a coherent scattering of the free carriers from the array of impurities; this is a two-ion process which thus produces a contribution of order x^2 . (ii) An incoherent scattering which is a single-ion process, proportional to x . In the particular case of a nondiluted ferromagnetic semiconductor ($x=1$), the coherent scattering goes through a maximum near T_c ,^{23,24} which gives rise to a peak of resistivity, slightly above T_c ,²⁴ observed experimentally. By analogy with the critical behavior of $\rho(T)$ in nondiluted ferromagnets, the peak of resistivity was also used to determine T_c in Ref. 8.

However, in a diluted semiconductor like $\text{Sn}_{1-x}\text{Mn}_x\text{Te}$ where $x^2 \ll 1$, the contribution of the coherent scattering becomes negligible, and the amplitude of the resistivity peak should vanish in this limit. As pointed out in Ref. 7, any direct relation between the peak of $\rho(T)$ and T_c in $\text{Sn}_{1-x}\text{Mn}_x\text{Te}$ is questionable. The fact that neither the amplitude of the peak nor its width is reproducible from one sample to another, at any given concentration x , also suggest that the peak is not a critical behavior of $\rho(T)$, contrary to the situation met in concentrated systems like Eu chalcogenides in the close vicinity of a transition be-

tween *homogeneous* paramagnetic and ferromagnetic phase. The peak observed in Refs. 7 and 8 might be due to a resonant scattering either on some impurity, or on ferromagnetic clusters being found in the intermediate superparamagnetic phase.

Since the incoherent scattering is the simple addition of the diffusion by individual impurities, it is sufficient to start from the one-ion Yosida Hamiltonian²⁵

$$H_I = \frac{1}{N} \sum_{\mathbf{k}, \mathbf{k}', \sigma} V c_{\mathbf{k}', \sigma}^\dagger c_{\mathbf{k}, \sigma} + \frac{1}{N} \sum_{\mathbf{k}, \mathbf{k}'} [(c_{\mathbf{k}', +}^\dagger + c_{\mathbf{k}, +} - c_{\mathbf{k}', -}^\dagger - c_{\mathbf{k}, -}) S_z^+ + c_{\mathbf{k}', +}^\dagger + c_{\mathbf{k}, -} S^- + c_{\mathbf{k}', -}^\dagger - c_{\mathbf{k}, +} S^+] \quad (20)$$

which describes the interaction between the free-carrier gas and a single magnetic ion of spin S . σ refers to the free-carrier spin polarization $+, -$. The first term is the local change in the crystal-field potential induced by the substitution of Sn by a Mn ion in the matrix. We note that the scattering problem has been solved formally in Refs. 9 and 25 for a more general interaction Hamiltonian allowing for a nonlocal and nonisotropic interaction J and V . Due to the lack of information concerning the structure of these quantities in the particular case of $\text{Sn}_{1-x}\text{Mn}_x\text{Te}$, however, we regard them as phenomenological parameters of our problem. We note that, in the end, we find $V > J$, in which case Koon *et al.*⁹ have shown that the results are not sensitive to this approximation of local and isotropic interactions in the limit $S \gg 1$.

The electrical resistivity can be deduced from the insertion, in the Boltzmann equation, of the transition rates computed from a perturbation expansion in the Born approximation. The third-order terms in H_I give rise to the Kondo effects. In $\text{Sn}_{1-x}\text{Mn}_x\text{Te}$, no Kondo effect can be detected, at least in the range of temperatures investigated ($T > 1.5$ K). In particular, the lowering of ρ near T_c cannot be imputed to a Kondo suppression due to an inelastic scattering of the free carriers by the magnetic Mn impurities, in contrast with the situation met in other materials.^{26,27} We thus admit that third-order terms are unimportant in our particular case, and we only consider the lowest-order terms (first Born approximation). The expression of the resistivity is then:⁹

$$\rho_M = \frac{m}{pe^2} \left[2\pi x V^2 D(E_F) + \frac{1}{2} \pi x J^2 D(E_F) (\langle S_z \rangle_\lambda^2 + S_l + S_t) - \frac{\pi x V^2 J^2 \langle S_z \rangle_\lambda^2 D(E_F)}{V^2 + \frac{1}{4} J^2 [\langle S_z \rangle_\lambda^2 + S_l + S_t]} \right] \quad (21)$$

with $D(E_F)$ the density of states per atom per spin direction. If $n(\omega) = (e^{\omega/(k_B T)} - 1)^{-1}$ is the Bose-Einstein factor, we define

$$S_{t,l} = \int_{-\infty}^{+\infty} \frac{d\omega n(\omega)}{k_B T} \gamma_{t,l}(\omega), \quad (22a)$$

where

$$\gamma_t(\omega) = \int_{-\infty}^{+\infty} \frac{dt}{2\pi} e^{-i\omega t} \langle S_-(0) S_+(t) \rangle_\lambda \quad (22b)$$

and

$$\gamma_l(\omega) = \int_{-\infty}^{+\infty} \frac{dt}{2\pi} e^{-i\omega t} \langle S_z(0) S_z(t) \rangle_\lambda, \quad (22c)$$

with the same conventional notations of Ref. 9. Actually, this expression of ρ is formally equivalent to Eqs. (2)–(7) in Ref. 9, except that the thermodynamic average of the quantum mean value of operators over the canonical ensemble, denoted $\langle \rangle$, have been replaced by $\langle \rangle_\lambda$, which represent the same quantity averaged over regions of the sample at the scale of λ , to take into account the finite value of the hole mean free path. For a homogeneous system at the scale of λ , i.e., when $\lambda \gg l$ with l the size of the ferromagnetic clusters or the ferromagnetic domains, the limit $\lambda \rightarrow \infty$ is valid so that $\langle \rangle_\lambda$ reduces to $\langle \rangle$, which quantity is homogeneous in space. This is the case implicitly envisioned in Ref. 9. In $\text{Sn}_{1-x}\text{Mn}_x\text{Te}$, however, the anomalous transport properties reported in the preceding section suggest that $\lambda \leq l$, in which case $\langle \rangle_\lambda$ does not reduce to $\langle \rangle$. The parameter λ is given by

$$\lambda = \frac{\hbar(3\pi^2)^{1/3}}{e^2} \frac{1}{\rho p^{2/3}}. \quad (23)$$

The variations of λ ($T = 10$ K) as a function of x are reported in Fig. 3 together with the variations of the mean distance \bar{R} between the magnetic ions. We note that $\lambda(T) \lesssim l(T)$ and the fact that λ is a decreasing function of temperature imply that the value of λ reported in Fig. 3 is a lower limit for the parameter l in the whole range of temperature of interest ($T < 10$ K). Figure 3 shows that λ is 1 order of magnitude larger than \bar{R} . On one hand, this

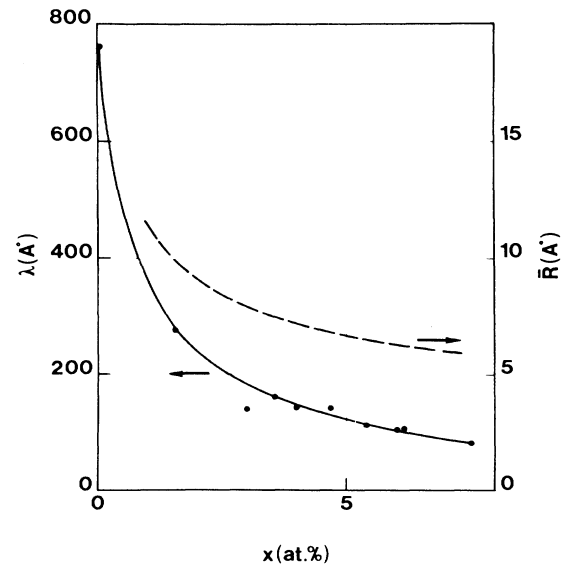


FIG. 3. Hole mean free path λ (solid curve left scale) and mean distance between Mn ions \bar{R} (dashed curve, right scale) as a function of x in $\text{Sn}_{1-x}\text{Mn}_x\text{Te}$.

result justifies the neglect of the cutoff effect of the hole mean free path on the RKKY coupling constant $J_{\text{eff}}(R_{ij})$.²⁸ Second, $l > \lambda$ implies that the ferromagnetic clusters embed few 10^5 magnetic ions at low temperatures, and $l \gg \bar{R}$ implies that a local molecular-field approximation may be used to derive the magnetic properties of the spins inside each cluster. We can then write, by analogy with Ref. 9:

$$\begin{aligned} \langle S_z(0)S_z(t) \rangle_\lambda &= \langle S_z^2 \rangle_\lambda - \langle S_z \rangle_\lambda^2, \\ \langle S_-(0)S_+(t) \rangle_\lambda &= \langle S_-S_+ \rangle_\lambda e^{-i\Omega_I t}, \end{aligned} \quad (24)$$

where Ω_I is the Larmor frequency of the impurity spin in the presence of the local effective field it is surrounded by; the effective field is the external field H_0 plus the internal molecular field

$$H_M = \frac{3k_B \bar{T}_c \langle S_z \rangle_\lambda}{g\mu_B S(S+1)}, \quad (25)$$

$$\rho_M = \frac{m\pi}{pe^2} D(E_F) \left\{ 2V^2 + \frac{1}{2}J^2 \{ \langle S_z^2 \rangle_\lambda + \beta\Omega_I [1 + n(\Omega_I)] \langle S_-S_+ \rangle_\lambda \} - \frac{V^2 J^2 \langle S_z \rangle_\lambda^2}{V^2 + \frac{1}{4}J^2 \{ \langle S_z^2 \rangle_\lambda + \beta\Omega_I [1 + n(\Omega_I)] \langle S_-S_+ \rangle_\lambda \}} \right\}. \quad (27)$$

If we note that

$$\begin{aligned} \langle S_z^2 \rangle_\lambda &= S(S+1) - \coth(\beta \langle S_z \rangle_\lambda \Omega_I / 2), \\ \langle S_-S_+ \rangle_\lambda &= 2n(\Omega_I) \langle S_z \rangle_\lambda. \end{aligned} \quad (28)$$

Equations (26)–(28) give the expression of ρ_M as a function of $\langle S_z \rangle_\lambda$.

B. Results

The determination of ρ as a function of T requires the knowledge of $\langle S_z \rangle_\lambda$. This parameter cannot be calculated since the distribution of exchange fields inside the material is unknown, but it can be deduced from magnetic measurements. We have shown that the magnetization $M(H_0)$ presents a component, easily saturated in a field $H_0 \sim 100$ G, which represents a Langevin-like magnetization associated to the alignment of the ferromagnetic clusters's spin polarization along the external field.⁶ This result led us to follow the following procedure: at any given temperature T , a magnetic field $H_0 = 5000$ G is applied to overcome macroscopic anisotropies which may appear in the material at low temperatures;²⁹ then H_0 is decreased down to $H_0 = 100$ G where the magnetization $M(H_0)$ is measured with a vibrating sample magnetometer. Such a magnetic field is still large enough to maintain the spin polarization of the weakly coupled ferromagnetic clusters aligned along H_0 , but is too small to modify significantly the distribution of effective fields and the amplitude of the local magnetization inside each cluster, so that we can write

with \bar{T}_c the freezing temperature of the spins inside the clusters, in the molecular-field approximation. T_c is then given by Eq. (15), at all concentration x (and not only for $x > x_c$), so that

$$\Omega_I = \frac{g\mu_B H_0}{\hbar} + \frac{3}{4} \frac{J^2 \Omega \rho x \langle S_z \rangle_\lambda}{\hbar E_F}, \quad (26)$$

the x concentration entering this equation is actually the Mn concentration inside the ferromagnetic clusters. Since $l \gg \bar{R}$, however, it is reasonable to assume that the Mn concentration is homogeneous at the scale of l , so that x reduces to the mean value entering the formula $\text{Sn}_{1-x}\text{Mn}_x\text{Te}$ (Microprobe analyses have shown that all our samples are homogeneous at the scale of the impact size of the electron beam, typically $1 \mu\text{m}$.) Taking Eqs. (22) and (24) into account, Eq. (21) is written as

$$\langle S_z \rangle_\lambda \simeq M(H = 100 \text{ G}) / (g\mu_B) \quad (29)$$

with $g = 2$ the Landé factor and μ_B the Bohr magneton, which value is used in Eqs. (26)–(28) to calculate ρ_M at temperature T .

The total resistivity of the samples, in the range $T < 10$ K where the phonon contribution is negligible, is written as

$$\rho = \rho_1 + \rho_M \quad (30)$$

with ρ_1 the contribution associated with the diffusion of the free carriers by nonmagnetic defects and impurities. The experimental values of ρ ($T = 10$ K) is reported as a function of x in Fig. 4. The linear dependence observed in this plot shows that ρ_M is proportional to x , which corroborates that interference effects between magnetic impurities is negligible. The dispersion of the experimental points in Fig. 4 is due to the fluctuations in the impurity concentration from one sample to another. In SnTe ($x = 0$), the residual resistivity is

$$\rho_1 = 2 \times 10^{-5} \Omega \text{ cm}. \quad (31)$$

ρ has been computed from Eqs. (26)–(28), (30) and (31), with J and V as variational parameters. The best fit, illustrated in Figs. 2 and 4, is obtained with

$$J = 0.4 \text{ eV}, \quad V = 1.55 \text{ eV}. \quad (32)$$

Since $\langle S_z \rangle_\lambda$ has been measured with temperature steps ~ 0.1 K within an accuracy $\sim 10^{-2}$, the theoretical values of $\rho(T)$ have been replaced by a continuous line in Fig. 2. This value of J is in agreement with the value deduced

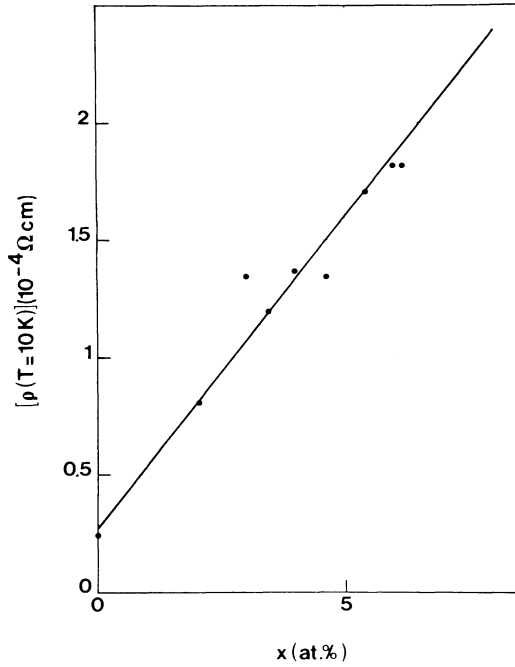


FIG. 4. Resistivity at $T=10$ K as a function of x in $\text{Sn}_{1-x}\text{Mn}_x\text{Te}$. Dots are experimental data. The solid line is theoretical.

from magnetic data in Eq. (18).

These values of J and V lead to a very good agreement between theory and experiment, for all the Mn concentrations investigated. The ferromagnetic ordering induces a decrease of the resistivity, as expected. A small decrease of $\rho(T)$ upon cooling is already observed above T_c , however, which corresponds to the fact that large ferromagnetic clusters are already formed above T_c , so that $\langle S_z \rangle_\lambda$ vanishes only at a temperature significantly larger than T_c . The decrease of $\rho(T)$ upon cooling in the reentrant phase, in good agreement with experimental data, is due to the fact that $\langle S_z \rangle_\lambda$ is larger in the reentrant phase than in the ferromagnetic phase, although the average bulk magnetization $\langle S_z \rangle$ in the limit $H \rightarrow 0$ is smaller or at most constant. This property is the consequence of the larger opening of the hysteresis cycle, with a larger deviation between field-cooled magnetization curves and virgin magnetization curve evidenced on these samples⁶ in the reentrant phase.

Following our procedure, we first determine $\langle S_z \rangle_\lambda$ from magnetic measurements, then we compute $\rho(T)$. In this context, these are magnetic properties which give evidence that $\langle S_z \rangle_\lambda$ increases upon cooling at T_r . Since, however, Eq. (27) defines a one-to-one reciprocal relation between $\langle S_z \rangle_\lambda$ and ρ , one can also consider that the decrease of ρ upon cooling is a transport property which, independently from magnetic measurements, gives evidence that $\langle S_z \rangle_\lambda$ increases upon cooling at T_r .

Finally, it should be noticed that the $\langle S_z \rangle_\lambda^2$ dependence of $\rho(T)$ is entirely contained in the third term of Eq. (27). It is precisely in the limit $(V/J)^2 \gg 1$ appropriate to $\text{Sn}_{1-x}\text{Mn}_x\text{Te}$ that this third term dominates the variations of ρ with temperature, in which case, for $S \gg 1$, Eq. (27) gives

$$\rho(T) = \rho(\infty) - \frac{\langle S_z \rangle_\lambda^2}{S^2} [\rho(\infty) - \rho(0)]. \quad (33)$$

$\rho(\infty)$ and $\rho(0)$ are given by Eq. (30) with

$$\begin{aligned} \rho_M(T \rightarrow 0) &= \rho_M(0) = \rho_0(4V^2 - J^2S^2), \\ \rho_M(T \rightarrow \infty) &= \rho_M(\infty) = \rho_0[4V^2 + J^2S(S+1)], \end{aligned} \quad (34)$$

with $\rho_0 = m\pi D(E_F)/(2pe^2)$. Equation 37 is just the extension of Eq. (19) to the case of inhomogeneous spin glasses where $\langle S_z \rangle_\lambda$ does not reduce to the bulk magnetization. The fact that Eq. (19) has been observed in canonical metallic spin glasses and that Eq. (37) applies in our case [the deviation with respect to Eq. (27) is smaller than 10%] suggests that the atomic potential perturbation due to the introduction of a magnetic ion in the host matrix is generally large, so that $(V/J)^2 \gg 1$ in the spin glasses investigated so far. $\text{Sn}_{1-x}\text{Mn}_x\text{Te}$ is no exception to this rule.

IV. DISCUSSION

Our model used to fit the resistivity curves of $\text{Sn}_{1-x}\text{Mn}_x\text{Te}$ differs from the prior work of Ghazali *et al.*⁸ in many aspects. First, no distinction has been made between $\langle \rangle$ and $\langle \rangle_\lambda$ in Ref. 8, assuming implicitly that $\lambda > l$. We have shown in this paper that the opposite situation $\lambda < l$ is met, and already discussed the consequences on the $\rho(T)$ curves. Second, the last term of Eq. (27) has been omitted in Ref. 8. This is a cross term between J and V which describes interference between the potential scattering and the non-spin-flip part of the exchange scattering.⁹

This term can be neglected only in the limit $V/J \rightarrow 0$, in which case the temperature dependence of ρ_M on temperature is due to the second term in Eq. (27). Even in this limit, Eq. (27) gives an expression of $\rho(\infty)$ which matches the result of Ref. 8, but gives an expression of $\rho(0)$ which differs from zero, at variance with the expression of $\rho(T)$ in Ref. 8. This disagreement arises because Ghazali *et al.* used the expression of the resistivity derived by de Gennes and Friedel²³ for ferromagnetic crystals ($x=1$), in which the contribution $\rho_0 J^2 \langle S_z \rangle^2$ is subtracted from Eq. (27). This procedure is justified in Ref. 23 because the term $\rho_0 J^2 \langle S_z \rangle^2$ corresponds to the scattering by the periodic part of the exchange potential. In a dilute material like $\text{Sn}_{1-x}\text{Mn}_x\text{Te}$, however, the magnetic ions are distributed randomly on the lattice and the spatial periodicity is lost, with the consequence that the de Gennes-Friedel theory does not apply. Equations (27), (32), and (34) correspond to the opposite approximation that the scattering of the free carriers by the magnetic ions is incoherent (which we have already justified in the preceding section) with no spatial correlations between the position of the Mn ions, which is justified, since $x \ll x_c$ and since $\rho(T=10\text{ K})$ is proportional to x in Fig. 4. As a consequence, if we omit the third term in Eq. (27) ($V/J \rightarrow 0$), like in Ref. 8, we find that the jump of resistivity $\Delta\rho = \rho(\infty) - \rho(0)$ is $\rho_0 S$, smaller than the value of Ref. 8 by a factor $S+1 = \frac{7}{2}$. The estimation of J entering the coefficient ρ_0 , deduced from a comparison between $\rho_0 S$ and the experimental estimation $\Delta\rho \simeq \rho(10\text{ K})$

$-\rho(T \rightarrow 0)$ is $J \sim 1$ eV, not compatible with magnetic experimental data. This is another form of evidence that V is large.

At last, $(V/J)^2 \gg 1$ implies that the last term in Eq. (27), not only cannot be omitted like in Ref. 8, but is the dominant term which yields the expression of $\Delta\rho$ given by Eq. (34), increased by a factor $(2S+1)/(S+1) = \frac{12}{7}$ with respect to the expression in Ref. 8, and a factor $2S+1=6$ with respect to $\rho_0 S$.

V. CONCLUSION

Metallic spin glasses investigated so far in the literature are homogeneous, i.e., the electron mean free path λ is larger than the size of the ferromagnetic clusters l , with the consequence that only domain rotation effects related to macroscopic anisotropies and demagnetizing fields

could be evidenced²⁹ in spin glass and reentrant spin-glass phases. Much lower densities of free-carrier gas can be obtained in degenerate semimagnetic semiconductors like $\text{Sn}_{1-x}\text{Mn}_x\text{Te}$, implying an increase of the radius R of the ferromagnetic cloud surrounding magnetic impurities, leading to an increase of l up to values $l > \lambda$. In such a case, the transport properties are a probe of the local magnetic properties, and give first evidence that the reentrant spin-glass phase is also characterized by an increase of local magnetization inside the larger nonsaturated ferromagnetic clusters or domains. The reentrant spin-glass phase corresponds to a situation where it becomes more favorable for the energy of the system to increase locally the magnetization, which is achieved at the expense of the bulk magnetization since the local axes of magnetization are blocked by magnetic anisotropies.

¹J. Friedel, *J. Phys. Rad.* **19**, 38 (1958); **23**, 692 (1962).

²J. Friedel, *Nuovo Cimento* **7**, 287 (1958).

³For a recent review, see, for example J. Spalek, *J. Magn. Magn. Mater.* **54-57**, 1207 (1986).

⁴J. Cohen, A. Globa, P. Mollard, H. Rodot, and M. Rodot, *J. Phys. (Paris), Colloq.* **29**, C4-143 (1968).

⁵M. Godhino, S. L. Tholence, A. Mauger, M. Escorne, and A. Katty, *Proceedings of the 17th International Conference on Ion Temperature Physics*, edited by U. Eckern, A. Schmid, W. Weber, and H. Wühl (North-Holland, Amsterdam, 1984).

⁶M. Escorne, M. Godhino, J. L. Tholence, and M. Mauger, *J. Appl. Phys.* **57**, 3424 (1985).

⁷M. Escorne and A. Mauger, *Solid State Commun.* **31**, 983 (1979).

⁸A. Ghazali, M. Escorne, H. Rodot, and P. Leroux-Hugon, *Magnetism and Magnetic Materials—1972 (Denver)*, Proceedings of the Conference on Magnetism and Magnetic Materials, edited by C. D. Graham, Jr. and J. J. Rhyne (AIP, New York, 1972), p. 1374.

⁹N. C. Koon, A. I. Schindler, and D. L. Mills, *Phys. Rev. B* **6**, 4241 (1972).

¹⁰The free carrier susceptibility appears here because the Coulomb correlations between the holes has been neglected. This approximation is not always valid in metals, but has been justified in the magnetic semiconductors; see for example A. Mauger, *Phys. Status Solidi B* **84**, 761 (1977).

¹¹See for example C. Kittel, *Quantum Theory of Solids* (Wiley, New York, 1967), p. 99.

¹²J. Sakurai, Y. Kubo, T. Kondo, J. Pierre, and E. F. Bertaut, *J. Phys. Chem. Solids* **34**, 1305 (1973).

¹³J. Souletic and R. Tournier, *J. Low Temp. Phys.* **1**, 95 (1969).

¹⁴T. Sone, *Solid State Commun.* **56**, 359 (1985).

¹⁵I. Riess and M. W. Klein, *Phys. Rev. B* **15**, 6001 (1977).

¹⁶B. B. Houston, R. S. Allgaier, J. Babiskin, and P. G. Siebenmann, *Bull. Am. Phys. Soc.* **9**, 293 (1964).

¹⁷H. Rakoto, J. C. Ousset, S. Senoussi, and I. A. Campbell, *J. Magn. Magn. Mater.* **46**, 212 (1984).

¹⁸S. Senoussi, *J. Phys. F* **10**, 2491 (1980).

¹⁹R. W. Schmitt and I. S. Jacobs, *J. Phys. Chem. Solids* **3**, 324 (1957); P. Marod, *Phys. Rev. Lett.* **79**, 1113 (1967); C. M. Hurd and J. E. Alderson, *Phys. Rev. B* **4**, 1088 (1971); S. P. McLister and C. M. Hurd, *ibid.* **20**, 1113 (1979); S. Senoussi, *J. Phys.* **42**, L35 (1981).

²⁰S. Senoussi and Y. Öner, *J. Appl. Phys.* **55**, 1472 (1984).

²¹Y. Yeshurun, M. B. Salamon, K. V. Rao, and H. S. Chen, *Phys. Rev. Lett.* **45**, 1366 (1980); G. Dublon and Y. Yeshurun, *Phys. Rev. B* **25**, 4899 (1982); M. A. Manheim, S. M. Bhagat, and H. S. Chen, *ibid.* **26**, 456 (1982); *J. Magn. Magn. Mater.* **38**, 147 (1983).

²²B. R. Coles, *Philos. Mag. B* **49**, L21 (1984); S. Senoussi and Y. Öner, *J. Magn. Magn. Mater.* **40**, 12 (1984); *J. Appl. Phys.* **55**, 1472 (1984).

²³P. G. de Genes and J. Friedel, *J. Phys. Chem. Sol.* **4**, 71 (1958).

²⁴M. Fisher and J. Langer, *Phys. Rev. Lett.* **20**, 665 (1968).

²⁵K. Yosida, *Phys. Rev.* **106**, 893 (1957).

²⁶I. Riess and A. Ron, *Phys. Rev. B* **4**, 4099 (1971).

²⁷K. Matho and M. T. Beal-Monod, *Phys. Rev. B* **5**, 1899 (1972).

²⁸See, for example, D. C. Mattis, *The Theory of Magnetism* (Harper and Row, London, 1965).

²⁹S. Senoussi, *Phys. Rev. B* **31**, 6086 (1985).